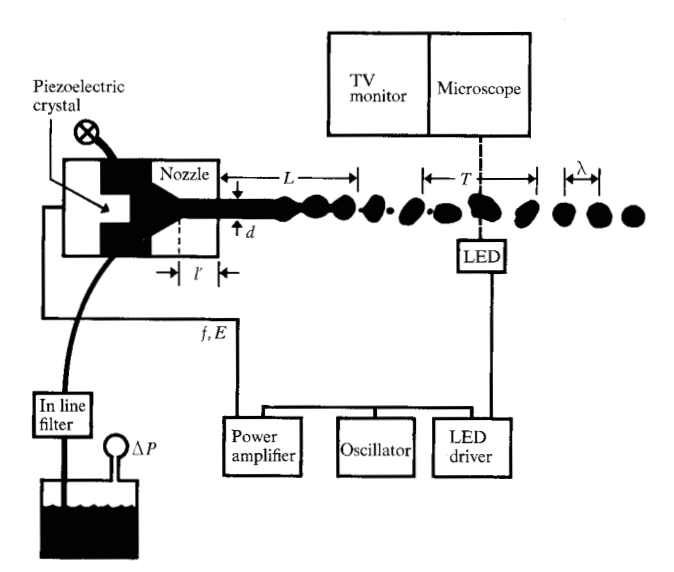
Dependence of Ink Jet Dynamics on Fluid Characteristics

Abstract: Measurements of jet velocity, separation length, and stream stability (freedom from random fluctuations in drop position) were made for several fluids, including two inks. The data were then compared with modified fluid flow and jet stability equations. In one case velocity is related to applied pressure drop through a flow equation that depends primarily on the shape and size of the nozzle and on fluid viscosity. In the other case Weber's equation is modified to include forced oscillation, so that separation length is related to the voltage applied to a piezoelectric crystal, to disturbance growth rate, and to velocity. These two equations were applicable to "normal" liquids (those having good stream stability) having viscosities between 0.9 and 4.3 grams/(second · meter) and dynamic surface tensions between 20 and 60 grams/s², but not to dilute solutions of a high molecular weight polymer, owing to their viscoelastic character. Furthermore, the stream stability of the polymer solutions was poor and depended inversely on concentration and molecular weight.

Introduction

In ink jet technology, uniformly spaced droplets are obtained by superimposing a periodic disturbance on a high velocity ink stream, which is pumped through a small orifice. Some of the drops are inductively charged as they break off from the main stream, and their trajectories are then modified by high voltage deflection plates. Printing is achieved with either the charged drops or the uncharged drops.

Figure 1 Ink jet apparatus.



Constant jet velocity and separation length must be maintained to print stably. Separation length (or time) affects charge synchronization and has a significant effect on drop placement. Velocity affects separation length, total deflection, and print height. The stream is also affected by satellite [1] drops (small secondary drops) and by poor stream stability (random fluctuations in drop position). Both satellite formation and poor stream stability lead to reductions in print quality.

This paper reports a study of the effects of ink physical properties, such as viscosity and surface tension, on jet velocity, separation length, and stream stability, for both ink and non-ink fluids. A high molecular weight polymer was added to both types of fluids to determine the effect of fluid elasticity on stream dynamics, although previous work [2, 3] had indicated that polymers are undesirable.

The dependence of velocity and separation length on ink properties was considered in terms of two equations, which were taken from the literature and modified for this flow problem. Stream stability was measured, and the results were compared directly with ink properties.

Jet flow equations

◆ Pressure-velocity

In the ink jet system used in this study (Fig. 1), ink is pumped from a reservoir through a filter into a conical entrance nozzle. Measurements and calculations indi-

258

cate that there is no pressure loss between the reservoir and the nozzle entrance. An equation for the pressure drop ΔP across a jet nozzle of length l' and diameter d was given by Sweet [4] as

$$\Delta P = \frac{\rho V^2}{2} + \frac{32\eta V l'}{d^2} + \frac{2\sigma_{\rm d}}{d},\tag{1}$$

where ρ is density, η viscosity, and σ_d dynamic surface tension of the fluid. This equation is valid [5] for the flow of a Newtonian liquid through a long uniform nozzle. For the short conical nozzle used in this work, it was necessary to modify Eq. (1) by adding the entry loss term

$$\frac{K\rho V^2}{2} + \frac{32\eta V\Delta l}{d^2},\tag{2}$$

where Δl is the excess viscous entry length and K is the entrance correction. This expression has been used by several researchers [6-9] to describe the flow of Newtonian liquids in the entry region of short tubes.

By combining Eqs. (1) and (2), we obtain for Newtonian liquids

$$\Delta P = \frac{\rho V^2}{2} + \frac{K \rho V^2}{2} + \frac{32 \eta V L_{\text{eq}}}{d^2} + \frac{2\sigma_{\text{d}}}{d}, \tag{3}$$

where $L_{\rm eq} = l' + \Delta l$.

This equation can be extended [10-13] to viscous "power law" fluids by modifying the viscous term in the usual manner. For viscoelastic fluids, Metzner [14] obtained an excess pressure term due to the fluid normal stresses.

• Separation length

Rayleigh [15] discovered that the breakup of a flowing liquid stream into a series of regularly spaced drops of wavelength λ (Fig. 1) is due to the surface tension of the fluid. Using linear perturbation theory, Rayleigh found that disturbances initially present in the stream grow exponentially $[\exp(\alpha t)]$, where α is the growth rate factor. For inviscid fluids $(\eta=0)$, $\alpha=0$ at $\lambda=\pi d$, then increases rapidly to a maximum at 4.51 d (Fig. 2), and slowly falls off with increasing λ .

Weber [16] extended Rayleigh's analysis to jets of viscous liquids and obtained the following equation for α :

$$\alpha = -\frac{3}{2\rho} \left(\frac{2\pi}{\lambda}\right)^{2} + \left\{\frac{9}{4} \left(\frac{\eta}{\rho}\right)^{2} \left(\frac{2\pi}{\lambda}\right)^{4} + \frac{\sigma_{d}a^{2}}{2\rho a^{3}} \left(\frac{2\pi}{\lambda}\right)^{2} \left[1 - \left(\frac{2\pi a}{\lambda}\right)^{2}\right]\right\}^{\frac{1}{2}}, \tag{4}$$

where a = d/2 is the stream radius. At low viscosities $[\eta < 10 \text{ gram/(s} \cdot \text{m})]$, the α vs λ/d curves obtained from Eq. (4) are similar (Fig. 2) to those obtained by Rayleigh for $\eta = 0$. However, at very high viscosities, the

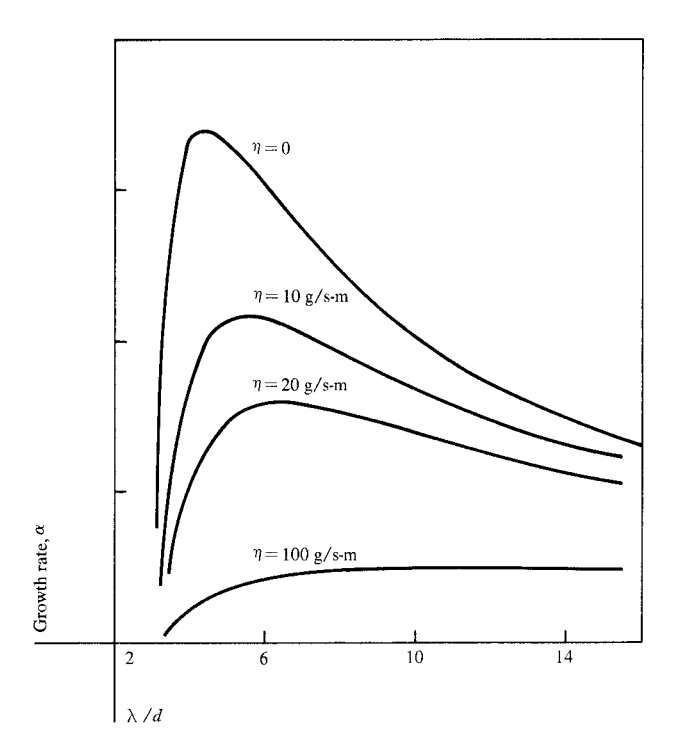


Figure 2 Dependence of theoretical growth rate α on λ/d and viscosity.

breakup is changed considerably, and regularly spaced drops may not be observed at all [4].

The separation length equation was also derived by Weber, who considered that the disturbance grows with the maximum rate; i.e., $I = I_0 \exp{(\alpha_{\max} t)}$, where I_0 is the disturbance amplitude at the jet origin. At the breakup point $(t=t^*)$, the disturbance equals the stream diameter [4]; $d = I_0 \exp{(\alpha_{\max} t^*)}$. At low velocity, separation length L is the product of velocity and breakup time:

$$L = Vt^* = \frac{V}{\alpha_{\text{max}}} \left[\ln \left(\frac{d}{I_0} \right) \right]. \tag{5}$$

For natural jets, Weber examined Haenlin's [17] data and obtained $\ln (d/I_0) = 12$; however, recent results [18, 19] indicate that this quantity depends on the fluid properties. At higher velocities, Weber obtained a maximum in the L vs V curve, which has been observed experimentally $\lceil 18-23 \rceil$.

In an ink jet printer, the externally excited jet breaks up into drops of wavelength λ , where λ is variable. In the present experiments, the jet was excited by a piezo-electric crystal in contact with the ink in the head. This produces a disturbance I_0 at the nozzle exit that is proportional to crystal drive voltage E [24, 25]. Thus, by

259

Table 1 Physical properties of fluids.

		Surface tension				
Run no.	Fluid	Density, ρ (g/cm^3)	σ , static (g/s^2)	$\sigma_{\rm d}$, dynamic (g/s^2)	Viscosity, η $(g/(s \cdot m))$	$\eta_{ m jet}/\eta$
1	Water 7/25/73	0.997	68	66?	0.89	_
2	Water 8/21/73	0.997	68	59	0.89	0.97
2 3	Water 9/13/73	0.997	56	59	0.89	0.95
4	15 % Carbowax 600	1.0227	57	57	1.866	1.03
5	15 % Carbowax 4000	1.0228	60	51	4.06	0.93
6	15 % Carbowax 1540	1.0221	56	50	2.62	0.99
7	1 % t-butyl alcohol	0.997	55	52	0.936	0.92
8	5 % t-butyl alcohol	0.990	44	37	1.11	0.99
9°	50 % t-butyl alcohol	0.904	23	20	4.29	0.95
10	$0.001 \% \text{ polyox } (MW = 5 \times 10^6)$	0.997	61	_	0.901	_
11	$0.01 \% \text{ polyox } (MW = 3 \times 10^5)$	0.997	58	_	0.907	_
12	$0.5 \% \text{ polyox } (MW = 2 \times 10^4)$	0.997	50	49	1.076	_
13	$0.0005 \% \text{ polyox } (MW = 5 \times 10^6)$	0.997	61	_	0.914	_
14	0.05 % Triton X-100	0.997	30	61	0.89	1.05
15	Soluble ink	1.035	_	60	1.76	1.12
16	Soluble ink	1.035	45?	60	1.76	1.07
17	Water	0.997	73	60	0.89	1.06
18	$0.01 \% \text{ polyox } (MW = 3 \times 10^5)$	0.997	42	_	0.929	
19	Soluble ink	1.035	40	57	1.76	1.05
20	Soluble ink + 0.01 % polyox $(MW = 3 \times 10^5)$	1.035	48	_	1.81	_
21	Soluble ink + 0.004 % polyox $(MW = 3 \times 10^5)$	1.035	38	44-67?	1.76	_
22	Dispersed ink	1.15	35	47	2.17	_
23	Soluble ink + 0.002 % polyox $(MW = 3 \times 10^5)$	1.035	42	58-68?	1.76	

aPartial nozzle clogging

substituting $I_0 = kE$ into Eq. (5), we obtain

$$L = \frac{V}{\alpha} \ln \left(\frac{d}{I_0} \right) = \frac{V}{\alpha} \left[\ln \left(\frac{d}{kE} \right) \right] = \frac{V}{\alpha} \left[\ln C - \ln E \right], \tag{6}$$

where k is a modified efficiency factor and C = d/k.

Sweet [4] considered another externally excited jet in which the initial disturbance is linear. This disturbance was then patched to the exponential disturbance of Rayleigh by matching derivatives, and a second equation for L was obtained:

$$L = \frac{V}{\alpha} \left[1 + \ln \left(\frac{V\alpha}{2\pi^2 f^2 k'} \right) - \ln E \right], \tag{7}$$

where k' is another efficiency factor.

Lee [1] obtained more complex equations for L by considering initial disturbances in which jet velocity or stream radius varies harmonically. One of Lee's results is similar to Sweet's equation, whereas the other is more complex.

Disturbance growth and separation length equations were obtained by Goldin, et al. [2] for linear viscoelastic fluids. For these fluids, they obtained the same equations for α (Eq. (4)) and L (Eq. (5)) as did Weber, but with the Newtonian viscosity replaced by the complex viscosity η^* , which represents the response to an oscillatory stress.

Experimental

• Apparatus

In the apparatus used in this study the ink is pumped through the nozzle and accelerated to velocity V by the pressure drop ΔP applied to the reservoir (Fig. 1). This steady pressure is modulated by the piezoelectric crystal. Crystal frequency f is chosen according to Rayleigh's theory such that f drops/second, regularly spaced, of wavelength λ are produced. The crystal oscillator also provided a signal to a light emitting diode (LED) driver, which drove a GaAs LED at one pulse per oscillation. The drops were observed stroboscopically with a microscope and on a television monitor.

• Fluids studied

Stream dynamics measurements were made on water and water solutions of t-butyl alcohol and Carbowax (trademark, Union Carbide Corp., New York, NY). Fluid viscosity was increased by adding 15% Carbowax (low molecular weight polyethylene glycol) to water; both viscosity and surface tension were varied by adding t-butyl alcohol to water. The effect of polymer concentration and molecular weight (MW) was studied by adding high molecular weight polyethylene oxide (polyox) to water and ink systems. The jet did not form properly

for Newtonian liquids with viscosity $\eta > 10$ g/(s·m), and stream breakup was unsynchronized for more concentrated polyox solutions.

A "soluble" ink and a "dispersed" ink were studied. The soluble ink contained a water soluble dye and miscellaneous additives, whereas the dispersed ink contained insoluble particles and a surfactant dispersed in water. A surface active agent, Triton X-100 (Trademark, Rohm and Haas Co., Philadelphia, PA for isooctyl phenol monoethylene glycol ether [26]) was also studied. The fluids tested are given in Table 1 with their properties.

• Measurements

Viscosity, surface tension, and density

Viscosity was measured using forward and reverse flow (for opaque inks) glass capillary viscometers [27]. The effect of shear rate was studied by putting the capillaries under pressure. For all the polyox solutions, viscosity was constant up to 20,000 s⁻¹ and never more than a few percent greater than that of the solvent (Table 1).

Static surface tension σ was determined with a du Nouy ring [28] and an overflowing vessel to prevent contamination. The surface tension data were obtained on samples after they were used in the system. The erratic values of σ obtained for water were apparently due to contamination by ink or cleaning solutions.

Pressure drop and velocity

The pressure drop applied to the reservoir was measured with a calibrated gauge. Accuracy was poorest at the lowest flow rates, where the gauge was difficult to read accurately. Volumetric flow rate Q was determined by collecting and weighing the stream.

Because the dispersed ink consistently clogged the nozzle and the in-line filter, data obtained on it were interpreted cautiously. The flow rate (at constant pressure) for two fluids was measured with and without the filter in place. No differences were noted, indicating a negligible pressure drop across the filter. However, after several hours of continuous operation, flow rate decreased slightly (about 2%) for some fluids, owing either to partial filter clogging or to a buildup of deposits in the nozzle itself.

The nozzle is mounted on a moveable x-y stage, whereas the LED, microscope, and television camera are fixed. Thus wavelength λ was measured directly by moving the stage and observing the position of the drops on the television monitor. Jet velocity V was then determined from the equation $V=\lambda f$ (see [4]), which is obtained from flow rate and the conservation of mass equations for incompressible fluids. The data fit the equation well, and values of V for each fluid were obtained from plots of λ vs 1/f.

Table 2 Parameters derived from pressure-flow rate data.

Run No.	Radius, a (cm)	Entrance factor, K	Equivalent length, L _{eq} (cm)	
Normal				
fluids				
2	0.00198	0.18	0.00768	
4	0.00198	0.25	0.00817	
5 3	0.00198	0.42	0.00737	
	0.00196	0.20	0.00751	
6	0.00196	0.27	0.00787	
7	0.00199	0.22	0.00731	
8	0.00199	0.28	0.00789	
	0.00189	0.36	0.00754	
14	0.00200	0.23	0.00835	
15	0.00200	0.29	0.00885	
16	0.00198	0.25	0.00852	
17	0.00199	0.29	0.00845	
19	0.00198	0.29	0.00837	
		average $= 0.007$		
Polyox				
solutions				
10	0.00199	0.13	0.0254	
11	0.00201	0.29	0.00946	
12	0.00197	0.24	0.00943	
13	0.00198	0.16	0.0142	
18	0.00201	0.25	0.0167	
20	0.00199	0.28	0.00943	
21	0.00197	0.20	0.00994	
23	0.00198	0.25	0.0105	

[&]quot;Partial clogging observed

Volumetric flow rate Q is related to velocity V by $Q = \pi a^2 V$; therefore, nozzle radius a was determined from the measured values of Q and V. The values of a were independent of flow rate and the fluid being studied (Table 2) except where partial nozzle clogging was present (run 9).

Figure 3 Breakup of normal and polymer solution jets.



Normal breakup



Polyox solution breakup

261

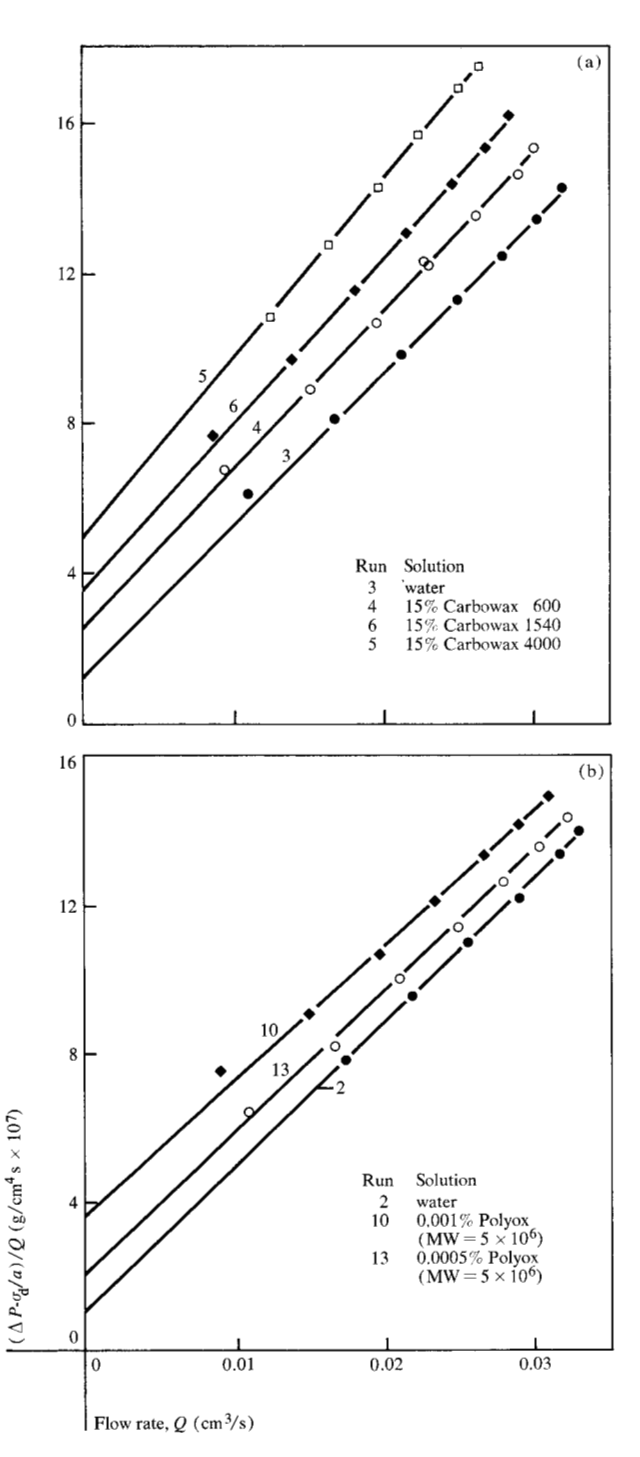


Figure 4 Test of Eq. (9). (a) Data on water and 15% Carbowax solutions; data on water and polyox solutions.

Separation length and stream stability

Separation length and stream stability were both measured using the LED and the microscope or television monitor. Separation length was measured by moving the x-y stage and observing the distance between the nozzle

exit and the breakoff point. The measurement was least accurate for the least stable fluids, because the breakoff could not be clearly distinguished.

Stream stability was measured 1.27 cm down from the nozzle at $\lambda = 0.0229$ cm and f = 100 kHz. The measurement consisted of increasing the voltage on the piezoelectric crystal until the drop image (as seen through the microscope) no longer became clearer. The minimum voltage required to get a time-stable, jitter-free stream was used as the measure of stream stability.

Dynamic surface tension

Drops, upon detachment from the jet, undergo a shape oscillation until they become spherical. The equation for this oscillation was developed by Rayleigh [15], who found that the period T is related to dynamic surface tension $\sigma_{\rm d}$ by

$$\sigma_{\rm d} = \frac{3\pi m}{8T^2} = \frac{3\rho \pi^2 a^2 \lambda}{8T^2} \,, \tag{8}$$

where $m = \rho \pi a^2 \lambda$ is the drop mass.

Period T was measured in the same way as wavelength. Normally two to three periods were visible, and values of $\sigma_{\rm d}$ with an accuracy of $\pm 10\%$ were obtained (Table 3) for most fluids. Values of $\sigma_{\rm d}$ for water (runs 1, 2, 3, 17) were more constant (59 \pm 2) than values of σ (57 to 73), which suffered from contamination problems. The low value obtained for $\sigma_{\rm d}$ for water is in agreement with Rayleigh's [15] reported measurements.

Due to the reduced stream stability of the polyox solutions (Fig. 3), it was difficult to observe a long enough oscillation period to make a reliable estimate for $\sigma_{\rm d}$ for these solutions. For runs 21 and 23, the measured values of $\sigma_{\rm d}$ were close to those obtained for the solvent ($\sigma_{\rm d}=59$). Therefore, the value of $\sigma_{\rm d}$ for the solvent (water or soluble ink) was used for the polyox solutions in further calculations.

For most fluids studied, $\sigma_{\rm d}$ was close to the static value. Both $\sigma_{\rm d}$ and σ were reduced (Table 1) as the concentration of t-butyl alcohol was increased. However, for the surfactant solution (run 14, Triton X-100), $\sigma_{\rm d}$ was similar to that of the solvent, water, whereas σ was much reduced.

Results and discussion

• Pressure dependence of flow rate

Normal fluids

The dependence of fluid velocity V on pressure drop and fluid physical properties $(\eta, \rho, \sigma_{\rm d})$ is predicted by Eq. (3). Because flow rate Q was the measured property, it was convenient to substitute Q in Eq. (3), giving

$$\frac{\Delta P - \sigma_{\rm d}/a}{Q} = \frac{\rho (1 + K)Q}{2\pi^2 a^4} + \frac{8\eta L_{\rm eq}}{\pi a^4},\tag{9}$$

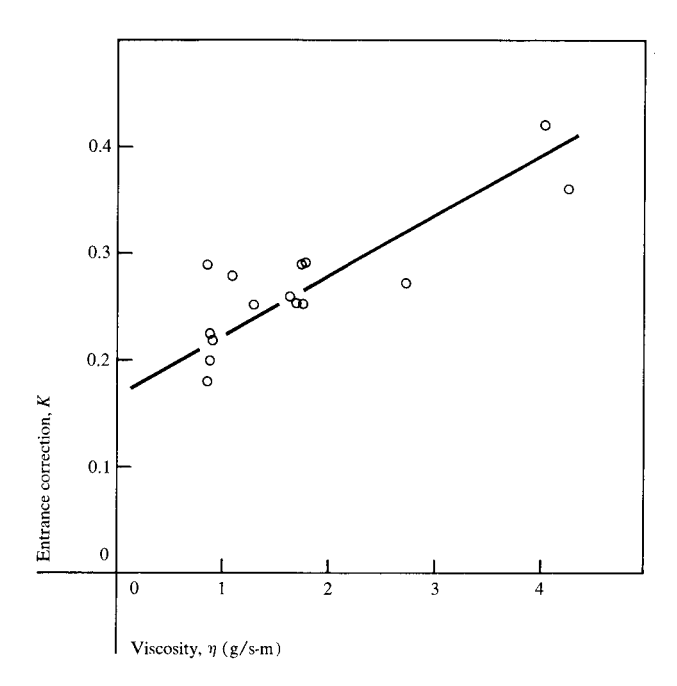


Figure 5 Dependence of entrance correction of normal fluids on viscosity.

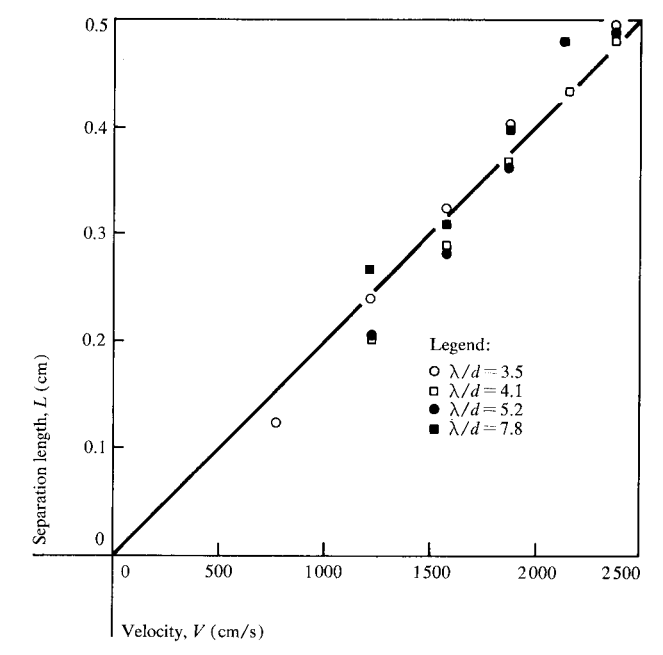


Figure 6 Separation length vs velocity for water.

where a was determined experimentally for each run (Table 2). The experimental data were then compared with Eq. (9) by plotting the quantity on the left side against Q, as shown in Fig. 4.

In general, the experimental data fit a straight line quite well. Deviations at high flow rates are believed due to pressure errors or to slight clogging. At the lowest flow rate, the data were often above the line (Fig. 4). These deviations may be due to pressure gauge errors (particularly at low pressure) or to failure of the jet to form properly at low velocity. This has been observed by other investigators [18-21], who did not consider it important. Therefore, deviations at low flow rates were ignored, and straight lines were drawn.

From the lines in Fig. 4, values of the entrance correction K and the equivalent length $L_{\rm eq}$ were obtained (Table 2). With normal fluids $L_{\rm eq}$ was constant at 0.00797 \pm 0.00049 cm. The measured length/diameter ratio was then equal to 2.00, which is in excellent agreement with the specified value and indicates that the excess length is zero for this nozzle. This result is in agreement with Rivas and Shapiro [7].

Because $L_{\rm eq}=l'=0.00797$ cm for normal fluids, the intercept of Fig. 4(a) can be used with Eq. (9) to obtain a value for the viscosity $\eta_{\rm jet}$, as measured in the jet flow. This was done for the normal fluids, and values of $\eta_{\rm jet}/\eta$ ranged from 0.93 to 1.12 (Table 1) for fluids whose viscosities varied from 0.9 to 4.3 g/(s·m). Therefore, from

Table 3. Illustrative data for evaluation of dynamic surface tension.

Fluid	Wavelength, λ (cm)	Velocity, V = (cm/s)	Oscillation period, T (µs)	Mass, m $(10^{-7}g)$	Dynamic surface tension, $\sigma_{ m d}$ (g/s^2)
water	0.0174	1730	62	2.12	64.9
water	0.0201	2010	70	2.46	59.1
water	0.0229	2290	75	2.81	58.9
water	0.0250	2510	78	3.08	59.6
soluble ink	0.0186	1850	70.6	2.38	56.3
soluble ink	0.0213	2100	74.2	2.72	58.1
soluble ink	0.0232	2300	76.8	2.97	59.4
soluble ink	0.0247	2450	81	3.16	56.7

a measurement of the jet flow properties $\Delta P, Q, V$, and $\sigma_{\rm d}$, a good estimate of fluid viscosity η is obtained for normal liquids.

The entrance correction factor K varied from 0.18 to 0.42 and increased with increasing η (Fig. 5). For normal liquids, the Reynolds Number, $N_{\rm Re}$ varied from 10 to 100 and for the jet flow was roughly proportional to $1/\eta$; therefore K is a function of $N_{\rm Re}$. This is in agreement with theoretical predictions [7].

The results indicate that Eq. (3) is sufficient to predict the velocity of a normal fluid in an ink jet nozzle. For the smooth, conical entrance head used in this study, the parameters in Eq. (9), K and $L_{\rm eq}$, are obtained from Fig. 5 and Table 2.

Liquids containing polymer additives

The data obtained on the solutions containing polyox (Fig. 4) also fit Eq. (9) quite well. However, $L_{\rm eq}$ was consistently greater than l' and was quite erratic (Table 2). Further, K was quite low (0.13-0.16) for the highest molecular weight polyox (5×10^6) and was more normal for the lower molecular weight polyox solutions.

The pressure drop data on the polyox solutions at high flow rates approach those for water (Fig. 4(b)). This is in marked contrast to data on viscous Carbowax solutions (Fig. 4(a)), which show increasing divergence at high flow rates. The "power law" fluid model predicts that the flow rate data should converge at high flow rates; however, measured viscosity changes were far too small to explain the large experimental deviations noted. Metzner's [14] viscoelastic theory does predict large entrance corrections, which were observed. However, they are due to normal stresses, which could not be measured in these dilute solutions.

The non-Newtonian viscosity and normal stresses are expected to increase with increasing polymer concentration [29]; however, the values of $L_{\rm eq}$ for these three concentrations (0.002, 0.004, and 0.01%) of polyox (MW = 3 × 10⁵) in the soluble ink clearly show a decrease in $L_{\rm eq}$ (Table 2) with increasing concentration. Therefore the intercept on Fig. 4(b), $L_{\rm eq}$, is definitely not a measure of fluid viscosity, as it was for the normal fluids.

• Separation length

Separation length L was determined over a wide range of velocities V and wavelengths λ by varying pressure drop ΔP and frequency f. Separation length for water increased nearly linearly with velocity (Fig. 6) for a wide variation in conditions. Deviations from linearity were probably due to variations in $\ln C$ with frequency. No maximum in the separation length was observed for any fluid. The measured separation lengths were short, due to the external driver. However, jet velocities were

high and, in many cases, were significantly higher than those obtained in previous experiments [18, 20, 21] in which maxima were noted. Therefore, a maximum in the L vs V curve is due to long separation lengths, which permit other breakup mechanisms to occur, rather than to a critical velocity.

Because the separation length data were nearly linear, Weber's theory should apply. Therefore, the data obtained on water were compared directly with Eqs. (6) and (7), which were developed for externally excited jets. The data fit the form of each equation; however, as the operating frequency and velocity were changed, the value of k in Eq. (6) varied by 35%, while the value of k' in Eq. (7) varied by 1000%. If Sweet's equation is correct, this large variation in k' is due to mechanical resonance. The experimental data do exhibit a small resonance near 70 kHz, but no change of 1000% was noted. One of Lee's [1] equations was inapplicable to this system, and the other yielded results similar to those obtained from Sweet's equation. Because the smallest variation in parameters was obtained with Eq. (6), we used it in subsequent analysis.

Determination of growth-rate
Simple linear theory yields the equation

$$\frac{L}{V} = \frac{1}{\alpha} \left[\ln C - \ln E \right],\tag{6}$$

for a synchronously driven jet. If V, f, and λ are held constant, then $\ln C$ and α are also constant, and they may be determined by measuring L as a function of $\ln E$. The data were taken in this manner, and the results (Fig. 7) yielded straight lines (with some scatter) for every fluid studied. From the slope of these lines, α was determined (Table 4) at discrete values of λ/d for most fluids.

The experimental values of α were then compared with those predicted by Eq. (4), using the experimentally determined values of λ , η , σ_d , and ρ . The need to use σ_a in calculating α was confirmed by the results obtained on run 14 (Triton X-100 in water), which were in much better agreement with experiment when $\sigma_d = 61 \text{ g/s}^2$ was used, rather than $\sigma = 30 \text{ g/s}^2$. The ratio $\alpha/\alpha_{\text{theory}}$ varied from 0.80 to 1.19 for all fluids (Table 4), including the polyox solutions. The scatter was greater for the polyox solutions due to the lower precision of the data. The experimental values of α varied by a factor of 3 as $\sigma_{\rm d}$ increased from 20 to 60 g/s² and λ/d was varied from 3.2 to 10. The variation in α with both σ_d and λ is well predicted by Weber's equation. The value of α (at constant λ/d) also decreased as the viscosity of the Carbowax solutions increased (Table 1), in qualitative agreement [30] with theory (Fig. 2). However, the scatter in the data was large, and the effects were too small to make a definitive comparison with theory.

Table 4 Evaluation of α from $\ln E \vee \ln L/V$ data.

Run no.	Fluid	Growth rate, $\alpha \times 10^{-2}$ (s^{-1})	Intercept, ln C	$\frac{\lambda}{d}$	$\frac{\alpha}{\alpha_{ ext{theor}}}$
1 1 1	water	288 285 251 187	8.1 8.4 8.1 6.4	4.12 4.18 5.68 7.84	0.96 0.95 0.88 0.82
4	15 % Carbowax 600	253	7.82	4.00	0.98
4		246	7.58	5.40	0.92
4		214	6.95	6.57	0.86
4		181	6.46	7.81	0.89
5	15 % Carbowax 4000	199	7.15	3.79	1.00
5		230	6.90	5.12	0.98
5		204	6.90	6.77	0.96
5		185	7.26	8.35	1.02
3	water	293	8.3	4.34	0.98
3		231	7.43	6.39	0.88
3		178	6.38	8.66	0.86
6	15 % Carbowax 1540	222 175	6.49 6.63	3.71 9.25	1.02 0.98
7	1 % t-butyl alcohol	268	8.84	4.22	0.99
7		265	9.02	4.81	0.97
7		183	7.82	7.40	0.85
7		160	7.04	10.1	0.95
8 8 8	5 % t-butyl alcohol	204 215 198 149	7.73 7.66 7.32 7.29	3.64 4.17 5.31 8.29	1.05 0.95 0.89 0.84
10	$0.001 \% \text{ polyox } (MW = 5 \times 10^6)$	294	10.19	4.20	1.00*
10		299	10.82	5.19	1.04*
10		264	9.36	6.50	1.04*
9	50 %-t-butyl alcohol	97	6.56	3.66	0.93
9		140	7.27	5.64	0.93
9		120	6.11	7.40	0.90
9		104	6.85	9.00	0.89
11 11 11 11 11	0.01 % polyox (MW = 3×10^{3})	340 324 226 242 255 170	14.7 14.3 10.6 11.7 12.9 8.85	4.26 5.02 5.20 5.80 7.09 8.09	1.19* 1.15* 0.81* 0.91* 1.09* 0.87*
12 12 12 12 12 12	0.5 % polyox (MW = 2×10^4)	158 263 254 204 187 159	7.49 7.63 6.98 7.78 7.82 6.64	3.37 4.27 5.46 6.61 7.79 9.51	0.94 0.98 0.98 0.88 0.90
13 13 13 13 13	0.0005 % polyox (MW = 5×10^6)	242 282 245 272 204 189	9.31 9.16 9.50 9.37 8.16 7.62	3.59 4.04 4.72 5.17 6.62 7.70	0.98* 0.96* 0.81* 0.92* 0.80*
14 14 14 14	0.05 % triton X-100	157 258 241 227 220	6.87 8.20 6.79 7.26 7.02	3.29 4.14 5.50 6.31 7.79	0.98 0.87 0.84 0.85 0.97
15	soluble ink	261	8.74	4.47	0.90
15		182	7.93	7.75	0.83
16	soluble ink	246	8.80	4.42	0.84
16		198	7.51	7.27	0.83
17	water water + 0.01 % polyox (MW = 3×10^5)	279	8.8	4.42	0.94
18		329	15.2	4.63	1.12*
19	soluble ink ink + 0.01 % polyox (MW = 3×10^5) ink + 0.004 % polyox (MW = 3×10^5)	262	8.62	4.68	0.94
20		266	16.9	4.61	0.97*
21		286	11.8	4.66	1.02*
22	dispersed ink	220	8.52	4.54	0.94
23	ink + 0.002 % polyox (MW = 3×10^5)	268	9.39	4.93	0.95*
23		247	8.82	5.66	0.92*

 $^{^*\}alpha_{\rm theory}$ calculated using $\sigma_{\rm d}$ of solution without polyox

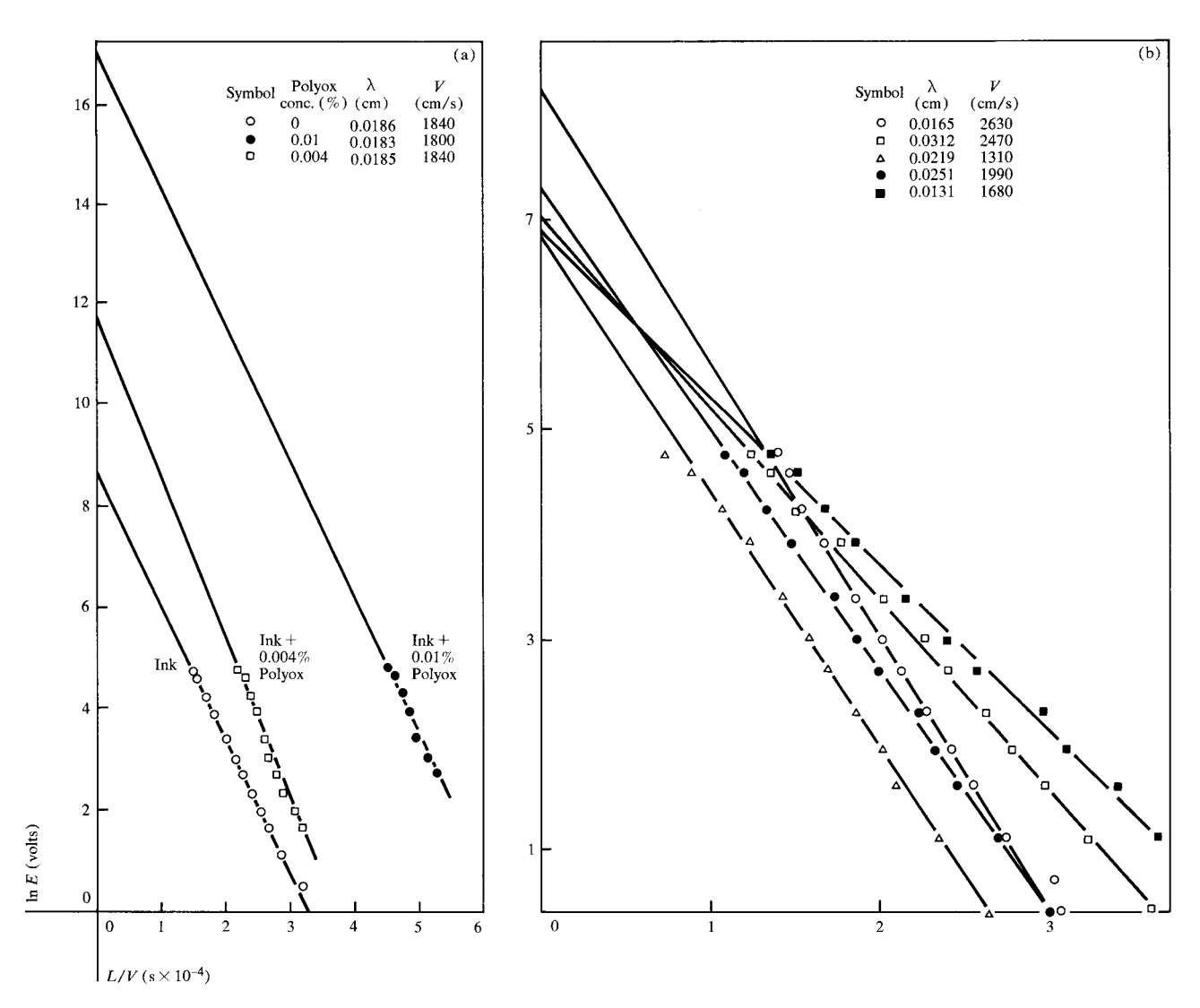


Figure 7 Test of Eq. (7), $\ln E \operatorname{vs} L/V$. (a) Data on soluble ink and polyox (MW = 3×10^5); (b) data on Triton X-100.

The results indicate that α is well predicted by Weber's theory for each fluid studied, including the polyox-containing fluids. The accuracy of α was $\pm 15\%$ and is comparable to that reported previously [18, 19, 21, 31].

Determination of $\ln C$ for normal fluids

In addition to α , the separation length equation also yields $\ln C$, which is a measure of head-driver efficiency. For normal liquids, $\ln C$ was found to be proportional to $\ln f$, specifically, $\ln C = \ln f - 4$, although the scatter (Fig. 8) was considerable. The observed proportionality $(k \propto 1/f)$ agrees with the theoretical prediction [24, 25] for the motion of a piezoelectric crystal operating in a viscous liquid far from resonance.

Because $\ln C$ is known for the normal liquids, a direct measure of separation length L or growth rate α is obtained from

$$\alpha = \frac{V}{L} \left[\ln C - \ln E \right] = \frac{V}{L} \left[\ln f - 4 - \ln E_0 \right]. \tag{10}$$

Hence, by operating the jet at constant E_0 and varying L,V, and f, values of α are obtained over a wide range of λ/d . For most of the normal fluids, data were taken in this manner, and curves of α vs λ/d were prepared (Fig. 9). The results show that the relation ($\ln C = \ln f - 4$) is capable of collapsing data obtained at different frequencies and velocities. These data were then compared with Weber's theory. The agreement (Fig. 9) is similar to that obtained (Table 4) for $\alpha/\alpha_{\rm theory}$ at discrete values of λ/d . For a given fluid, the agreement depends on how close the $\ln C$ values are to the $\ln f - 4$ line (Fig. 8). These results indicate a minor dependence of $\ln C$ on σ , $\sigma_{\rm d}$, and η . However, because of the complex dependence of $\ln C$ on frequency (Fig. 8), the precise effect of fluid properties was not determined.

The accuracy of the separation length prediction was $\pm 25\%$ and was valid over a very wide range of operating conditions. The prediction of L was less accurate than that of α because of the mechanical resonances of this particular head.

Values of In C for polymeric fluids

Values of $\ln C$ for the solutions containing polyox were also obtained from Eq. (6). They were much greater (Table 4) than those for the normal fluids, and the frequency dependence (Fig. 8) was no longer evident. These large values of $\ln C$ were due to the long separation lengths (Fig. 7(b)), which resulted from the presence of liquid strands (Fig. 3) between the drops. Stranding and long separation lengths were previously noted by Goldin, et al. [2] and Gordon, et al. [3] for other high molecular weight polymer solutions. The results obtained on the soluble ink with added polyox (MW = 3×10^5) indicates that $\ln C$ increases linearly with increasing polyox concentration (Fig. 10(a)). The value of $\ln C$ also increased as the concentration or molecular weight of polyox in water increased.

These long separation lengths indicate that disturbances of greater amplitude [3] are required to disrupt polymer solutions. Drop stranding apparently [2, 3] prevents the surface tension from breaking up the jet and leads to an elastic type breakup in which the strands are finally broken by stretching. This type of breakup is not very predictable, because it depends strongly on the polymer concentration (Fig. 10(a)) and has also been observed [2, 3] to be degraded by recirculation through the jet. Because of the uncertainty in the actual breakoff point, drop synchronization (required for stable printing) is much more difficult to maintain for polymer solutions.

· Stream stability

Stream instability is jitter or noise in the ink stream as seen stroboscopically with a LED synchronized with the drop rate. Stability, the converse of instability, is measured in volts applied to the piezoelectric crystal to produce a stable stream. This measurement is somewhat subjective; however, with a given operator, head, and driver, reproducible results are obtained.

Normal liquids

The stream stability results are presented in Table 5. Normal liquids are defined as all liquids that require stream stability voltages less than 4 volts. For these liquids, drop synchronization and jet breakup were observed at voltages below 1 volt; however, the driving signal was noisy and jitter in the stream was noted. By increasing the piezoelectric driver voltage to 4 volts, jitter ceased completely, and no further improvements were noted at higher voltages. The normal liquids in-

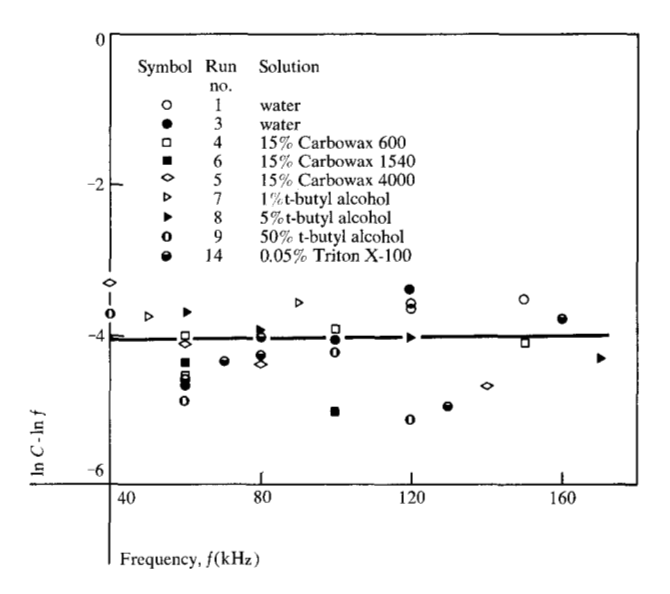


Figure 8 Values of $\ln C - \ln f$ vs frequency for normal fluids.

Figure 9 Experimental and theoretical growth rate vs λ/d for 15% Carbowax 1540.

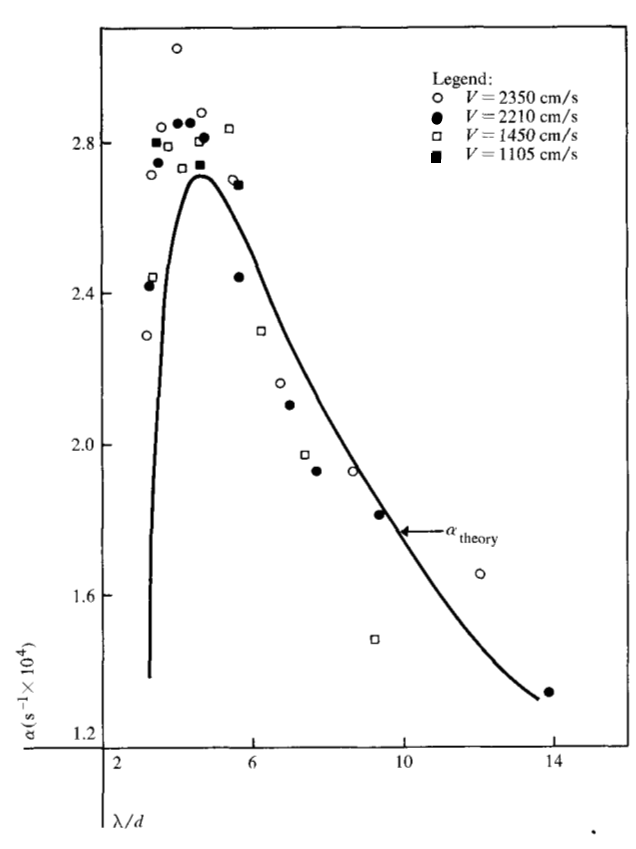


Table 5 Stream stability of different types of fluids.

Fluid	Stability (volts)	Notes
Normal fluids		
water	4	
water + t-butyl alcohol	≤4	
water + Carbowax (600, 1540, 4000)	≤4	
water + Triton X-100	≤4	
soluble ink	4	
Moderately stable fluids		
dispersed ink	10-30	nozzle clogging
soluble Ink + 0.002 % polyox (MW = 3×10^5)	10	
Unstable fluids		
soluble ink + 0.004 % polyox (MW = 3×10^5)	40	
soluble ink + 0.01 % polyox (MW = 3×10^{5})	70	
water + 0.01 % polyox $(MW = 3 \times 10^5)$	80	
water + 0.01 % polyox $(MW = 5 \times 10^6)$	>160	breakup not visible

cluded water, the soluble ink, the Carbowax solutions, the t-butyl alcohol solutions, and the Triton X-100 solution. In some cases, the stability data of normal liquids were obtained near the separation point. The stability data of other normal liquids did not change when the observation position was moved to 2.5 cm downstream from the nozzle; therefore, the data obtained at the separation point are believed to be correct.

These results indicate that stream stability is unaffected by changes in viscosity, surface tension, or dynamic surface tension over the ranges studied. Good stability was obtained with a surfactant solution (Triton X-100) and with a low surface tension fluid (50% t-butyl alcohol), which yielded very long separation lengths.

Polymer solutions and dispersions

Stream stability data on these fluids are also presented in Table 5. Moderate stability (6-30 volts) was obtained for the dispersed ink and a solution of 0.002% polyox $(MW = 3 \times 10^5)$ in the soluble ink. Very poor stability (>30 volts) was observed for polyox solutions of higher concentration or molecular weight.

For solutions of polyox $(MW = 3 \times 10^5)$ in the soluble ink, stability decreased linearly (Fig. 10(b)) with the polyox concentration. The separation length data also yielded a linear relation between $\ln C$ and concentration (Fig. 10(a)). Therefore, a plot was made of stability against $\ln C$ (Fig. 10(c)), and this also was linear. Hence, there is a direct relationship between stream stability and separation length for polyox solutions.

The results obtained by Goldin, et al. [2] and Gordon, et al. [3] on polyacrylamide solutions indicate that long separation lengths, drop stranding, and reduced stream stability are also observed for these solutions.

Therefore, stream stability is reduced by the presence of a high molecular weight polymer. Apparently, the polymer damps out the pressure wave much more severely than in normal liquids, leading to large values for $\ln C$ and resultant poor stream stability.

The dispersed ink was subject to serious clogging problems. It is believed that the clogging as well as the reduced stability were due to the presence of large particles in the dispersion. A more concentrated dispersion appeared even less stable; however, it clogged so quickly that stability data could not be obtained.

The stability results obtained on the polyox solutions appear to apply generally to high molecular weight polymers. However, it is unclear that dispersed inks exhibit reduced stability. Certainly, stream stability is reduced much more by the presence of a small concentration of high molecular weight polymer than it is by a much higher concentration of dispersed particles.

Summary and conclusions

The effects of fluid physical properties on ink jet velocity V, separation length L, and stream stability were studied for several inks and other fluids. Data were analyzed in terms of two equations, obtained by modifying and extending those used in fluid flow and ink jet theory. These equations were suitable for predicting the velocity and separation length for normal fluids having viscosities between 0.9 and 4.3 g/(s·m) and dynamic surface tensions $\sigma_{\rm d}$ between 20 and 60 g/s², where $\sigma_{\rm d}$ was determined from the jet flow itself.

The value of V depends primarily on applied pressure drop ΔP , nozzle diameter d, equivalent nozzle length $L_{\rm eq}$, and the entrance shape factor K. The value of L

C. A. BRUCE

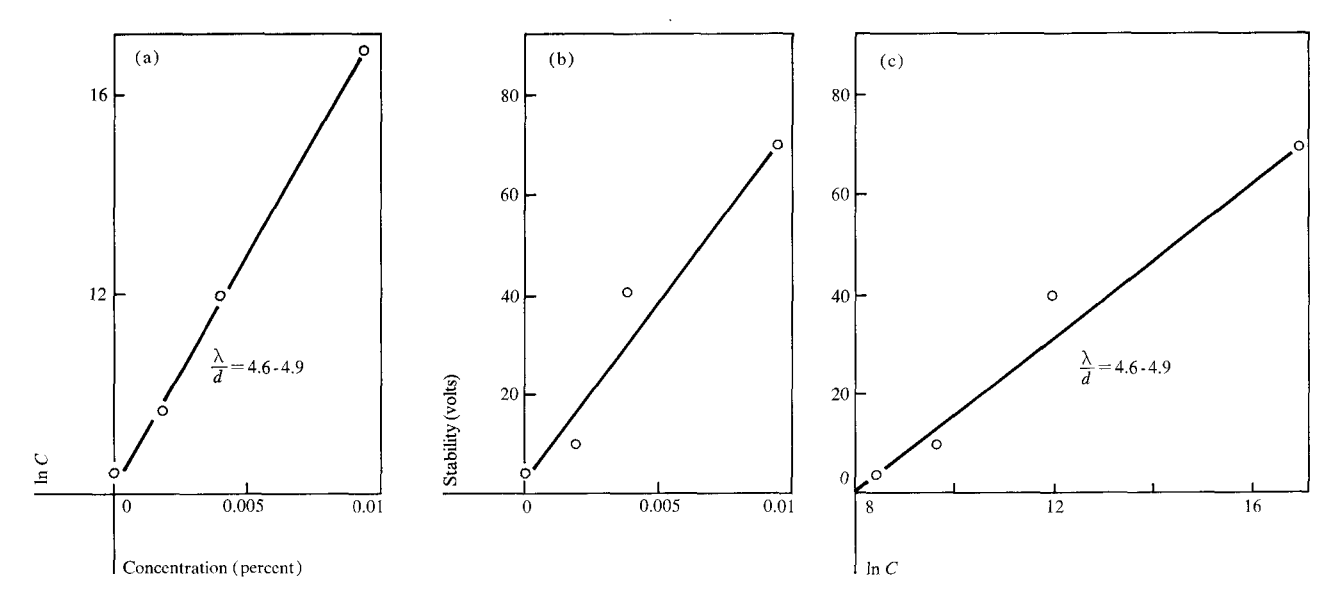


Figure 10 Soluble ink and polyox (MW = 3×10^5). (a) ln C vs concentration; (b) stability vs concentration; (c) stability vs ln C.

depends on V, the piezoelectric crystal voltage E, the efficiency factor $\ln C$, and the disturbance growth rate α . For the flow of normal fluids in a conical entrance head, $\ln C = \ln f - 4$, $L_{eq} = l'$ (the actual length), and K = 0.18 to 0.42; the latter increases with increasing viscosity. For all fluids studied, growth rate α depended on $\sigma_{\rm d}$, η , and the jet wavelength, in full accordance with Weber's theoretical prediction (Eq. 4). For higher viscosity fluids, jet velocities were quite low, and Weber's equation may not be applicable [30]. The predictions of V and L were accurate to within $\pm 10\%$ and $\pm 25\%$, respectively. If V and L are measured directly, the equations can be inverted to determine η and α for normal fluids with similar precision.

The two equations were inapplicable to dilute solutions of high molecular weight polyethylene oxide (polyox) in water and in the soluble ink, because both $L_{\rm eq}$ and ln C clearly depended on the polymer concentration. The viscous "power law" fluid model was also inadequate to explain the observed behavior of these solutions.

Stream stability was excellent for normal liquids and was independent of the fluid viscosity and surface tension over the range studied. The stability of the polyox solutions was poor and depended inversely on the polymer concentration and molecular weight and was directly related to the long separation lengths observed. The dispersed ink clogged badly and also exhibited reduced stream stability.

Acknowledgments

The author is grateful for the assistance of T. L. Baiko in the experimental and analytical portions of the work. The dispersed ink was supplied by Z. Kovac, and the soluble ink by D. L. Elbert. The head and driver were supplied by K. Chaudhari. Many helpful discussions and much encouragement were provided by M. Cantow, Y. Moradzadeh, and M. Tinghitella.

References

- 1. H. C. Lee, "Drop Formation in a Liquid Jet," IBM J. RES. Develop. 18, 364 (1974).
- M. Goldin, J. Yerushalmi, R. Pfeffer, and R. Shinnar, "Breakup of a Laminar Capillary Jet of a Viscoelastic Fluid," J. Fluid Mech. 38, 689 (1969).
- 3 M. Gordon, J. Yerushalmi, and R. Shinnar, "Instability of Non-Newtonian Jets," *Trans. Soc. Rheol.* 17, 303 (1973).
- R. G. Sweet, "High Frequency Oscillography with Electrostatically Deflected Ink Jets," *Technical Report* 1722-1, Stanford Electronics Laboratories, Stanford, CA, 1964.
- H. Schlichting, Boundary Layer Theory, 4th ed., McGraw Hill Book Company, Inc., New York, 1960.
- 6. M. Collins and W. R. Showalter, "Laminar Flow in the Inlet Region of a Straight Channel," *Phys. Fluids* 5, 1122 (1962).
- M. A. Rivas, Jr., and A. H. Shapiro, "On the Theory of Discharge Coefficients for Rounded Entrance Flowmeters and Venturis," *Trans. ASME* 78, 489 (1956).
- 8. N. D. Sylvester and S. L. Rosen, "Laminar Flow in the Entrance Region of a Cylindrical Tube," *AIChE J.* **16**, 964 (1970).
- 9. G. Astarita and G. Greco, "Excess Pressure Drop in Laminar Flow Through Sudden Contraction," *Ind. Eng. Chem. Fundam.* 7, 27 (1968).
- D. C. Bogue, "Entrance Effects and Prediction of Turbulence in Non-Newtonian Flow," Ind. Eng. Chem. 51, 874 (1959)
- M. Collins, and W. R. Schowalter, "Behavior of Non-Newtonian Fluids in the Entry Region of a Pipe," AIChE J. 9, 804 (1963).
- G. Astarita, G. Greco, Jr., and L. Peluso, "Excess Pressure Drop in Laminar Flow Through Sudden Contraction: Non-Newtonian Liquids," *Ind. Eng. Chem. Fundam.* 7, 595 (1968).

- M. Collins and W. R. Schowalter, "Behavior of Non-Newtonian Fluids in the Inlet Region of a Channel," AIChE J. 9, 98 (1963).
- A. B. Metzner, E. A. Uebler, and C. F. Chan Man Fong, "Converging Flows of Viscoelastic Materials," AIChE J. 15, 750 (1969).
- Lord Rayleigh, The Theory of Sound I & II, Dover Publications, Inc., New York, 1945.
- cations, Inc., New York, 1945.

 16. C. Weber, "Zum Zerfall eines Flüssigkeitsstrahles," Z. Angew. Math. Mech. 11, 136 (1931).
- A. Haenlein, Technical Memorandum No. 659, National Advisory Committee on Aeronautics, Washington, DC (1932).
- R. P. Grant and S. Middleman, "Newtonian Jet Stability," AICHE J. 12, 669 (1966).
- R. W. Fenn, III, and S. Middleman, "Newtonian Jet Stability: The Role of Air Resistance," AIChE J. 15, 379 (1969).
- 20. S. W. J. Smith and H. Moss, "Experiments with Mercury Jets," *Proc. Roy. Soc.* A-93, 373 (1917).
- 21. E. Tyler and E. G. Richardson, "The Characteristic Curves of Liquid Jets," *Proc. Phys. Soc.* 37, 297 (1925).
- A. C. Merrington and E. G. Richardson, "The Break-up of Liquid Jets," Proc. Phys. Soc. 59, 1 (1947).
- E. G. Richardson, "Mechanism of the Description of Liquid Jets," Appl. Sci. Res. A4, 374 (1954).
- W. G. Mason, Physical Acoustics and the Properties of Solids, D. Van Nostrand Co., Inc., Princeton, New Jersey, 1958.

- Technical Aspects of Sound II, edited by E. G. Richardson, Elsevier, London, 1957.
- D. A. Netzel, G. Hoch, and T. I. Marx, "Adsorption Studies of Surfactants at the Liquid-Vapor Interface," J. Colloid Sci. 19, 774 (1964).
- J. R. Van Wazer, J. W. Lyons, K. Y. Kim, and R. E. Colwell, Viscosity and Flow Measurement, Interscience Publishers, Inc., New York, 1963.
- 28. A. W. Adamson, *Physical Chemistry of Surfaces*, Interscience Publishers, Inc., New York, 1967.
- C. Bruce, and W. H. Schwarz, "Rheological Properties of Ionic and Nonionic Polyacrylamide Solutions," J. Poly. Sci. A27, 909 (1969).
- B. J. Meister, and G. F. Scheele, "Generalized Solution of the Tomotika Stability Analysis for a Cylindrical Jet," AIChE J. 13, 682 (1967).
- R. J. Donnelly and W. Glaberson, "Experiments on the Capillary Instability of a Liquid Jet," Proc. Roy. Soc. A-290, 547 (1965).

Received June 20, 1975; revised December 5, 1975

The author is located at the IBM Research Division Laboratory, Monterey and Cottle Roads, San Jose, California 95193.